BIOCHEMISTRY
including biophysical chemistry & molecular biology

Article

pubs.acs.org/biochemistry

Characterizing the Dynamics of α-Synuclein Oligomers Using Hydrogen/Deuterium Exchange Monitored by Mass Spectrometry

Simon Mysling,[†] Cristine Betzer,[‡] Poul H. Jensen,[‡] and Thomas J. D. Jorgensen*,[†]

[†]Department of Biochemistry and Molecular Biology, University of Southern Denmark, 5230 Odense M, Denmark

[‡]Department of Biomedicine and Danish Research Institute of Translational Neuroscience (DANDRITE), Aarhus University, DK-8000 Aarhus C, Denmark

Supporting Information

ABSTRACT: Soluble oligomers formed by α-synuclein (αSN) are suspected to play a central role in neuronal cell death during Parkinson's disease. While studies have probed the surface structure of these oligomers, little is known about the backbone dynamics of αSN when they form soluble oligomers. Using hydrogen/deuterium exchange monitored by mass spectrometry (HDX-MS), we have analyzed the structural dynamics of soluble αSN oligomers. The analyzed oligomers were metastable, slowly dissociating to monomers over a period of 21 days, after excess monomer had been removed. The C-terminal region of αSN (residues 94−140) underwent isotopic exchange very rapidly, demonstrating a highly dynamic region in the oligomeric state. Three regions (residues 4−17, 39−54, and 70−89) were strongly protected against isotopic exchange in the oligomers, indicating the presence of a stable hydrogen-bonded or solvent-shielded structure. The protected regions were interspersed by two somewhat more dynamic regions (residues 18−38 and 55−70). In the oligomeric state, the isotopic exchange pattern of the region of residues 35−95 of αSN corresponded well with previous nuclear magnetic resonance and electron paramagnetic resonance analyses performed on αSN fibrils and indicated a possible zipperlike maturation mechanism for αSN aggregates. We find the protected N-terminus (residues 4−17) to be of particular interest, as this region has previously been observed to be highly dynamic for both monomeric and fibrillar αSN. This region has mainly been described in relation to membrane binding of αSN, and structuring may be important in relation to disease.

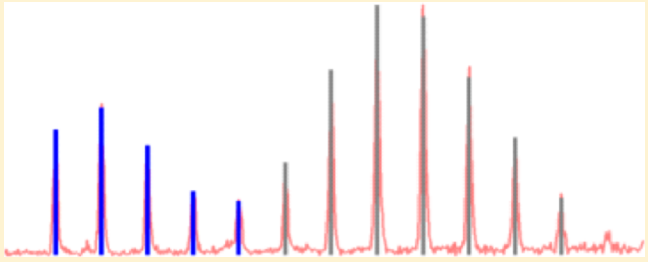

Parkinson's disease (PD) is a neurodegenerative disorder characterized by neuronal cell death and the formation of intraneuronal fibrillar inclusions (Lewy bodies) in the substantia nigra pars compacta and other brain regions.[1] Aggregated α-synuclein (αSN) is the predominant protein in Lewy bodies. The exact cause of neuronal cell death is still unknown, but soluble oligomeric aggregates of αSN have been proposed as promoters of neuronal cell death in relation to the disease.[2] This is supported by the point mutations in αSN (A30P, E46K, A53T, and the recently identified H50Q, G51D, A18T, and A29S) leading to different forms of PD, of which A30P, E46K, and A53T have been shown to have higher propensity to aggregate than the wild type.[3−8] αSN monomers are generally regarded as intrinsically disordered proteins.[9,10] The protein can aggregate in a concentration-dependent manner, and Lashuel et al. have reported that soluble oligomers could be isolated from concentrated αSN solutions.[11] The isolated soluble oligomers were structurally heterogeneous, generally adopting annular structures upon being investigated by electron microscopy (EM).[11] Similar findings regarding the structure and heterogeneity of isolated αSN oligomers have also been reported in studies using atomic force microscopy (AFM).[12,13] Recently, αSN oligomers adopting a similar circular wreath-shaped structure have been observed in solution using small-angle X-ray scattering (SAXS).[14] While the surface of αSN oligomers has been probed extensively, little is known about the backbone structure adopted by αSN when they form soluble oligomers. Of particular interest is the finding that the progression of αSN from its monomeric state toward oligomeric and fibrillar aggregates was accompanied by a loss of α-helical structure with a corresponding increase in the level of β-sheet structure, possibly indicating the formation of a fibril-like β-sheet fold during oligomer assembly.[12]

Hydrogen/deuterium exchange monitored by mass spectrometry[15,16] (HDX-MS) allows for the analysis of protein conformational dynamics, probing solvent exposure and hydrogen bonding of backbone amides. Deuterium uptake can be compared in intact proteins (global analysis) to reveal the presence of multiple conformational states, and following proteolytic digestion (local analysis) to identify regions that exhibit increases or decreases in their level of dynamic behavior upon comparison of the two conformations.[17] HDX analysis has proven to be a valuable technique for characterizing the structure and dynamics of aggregates formed by proteins

Received: July 11, 2013
Revised: November 5, 2013
Published: November 5, 2013

dx.doi.org/10.1021/bi4009193 | *Biochemistry* 2013, 52, 9097−9103

involved in diseases related to amyloid formation, such as the Aβ peptide[18−20] and amylin,[21] using both MS and NMR detection.[22−25] The HDX characteristics of fibrils formed by wild-type and mutant αSN have also previously been investigated.[26−28] In the study presented here, we examine the stability and structure of soluble αSN oligomers using HDX-MS. The heterogeneous nature of such dynamic oligomers makes them challenging to analyze by traditional spectroscopic techniques, such as NMR, as these methods yield population-average data. MS analysis of deuterium-labeled samples, however, can readily resolve individual populations arising from such heterogeneity, making it a useful analysis method when it is applied to such systems. Our HDX-MS experiments demonstrate similarities between oligomers and fibrils but interestingly also highlight the presence of an N-terminal region that is protected against isotopic exchange in the oligomers, indicating a structuring that could be a target for future oligomer-specific agents.

EXPERIMENTAL PROCEDURES

Materials and Reagents. Deuterium oxide (D_2O) of 99.9% isotopic purity was obtained from Cambridge Isotope Laboratories (Andover, MA). Phosphate-buffered saline (PBS) buffer (0.01 M phosphate buffer, 0.0027 M potassium chloride, and 0.137 M sodium chloride) was prepared from Sigma (St. Louis, MO) PBS tablets. For sample digestion, 5 μg/μL pepsin solutions in 10 mM HCl were prepared. αSN was expressed in *Escherichia coli*; cell lysates were precipitated in ammonium sulfate and resuspended, and αSN was purified using anion exchange, as described by Conway et al.[9]

Sample Preparation. Oligomerization of αSN was conducted as described by Lashuel et al.,[11] with a few modifications. In brief, αSN was dissolved to a concentration of 10 mg/mL (690 μM) in PBS, incubated on ice for 30 min, and centrifuged at 16000*g* and 4 °C for 5 min to remove insoluble particles. Oligomers were purified using gel filtration, an Amersham Superdex 200 HR 10/30 column (GE Healthcare Biosciences, Piscataway, NJ), PBS as the elution buffer, and a flow rate of 0.5 mL/min, giving a yield of 0.5−1%. To increase the oligomer concentration, a centrifugal filter unit was used according to the manufacturer's instructions (Amicon ultracel 10k). The final oligomer solutions had a concentration of ∼14 μM and were kept unfrozen, on ice, at all times prior to isotopic labeling.

Deuterium Labeling. Isotopic exchange of monomeric and oligomeric αSN was initiated by 10-fold dilution in deuterated PBS (pD 7.8, value corrected for isotope effect) to a final D_2O content of 90% (v/v) and 1.4 μM αSN. Exchanges were performed at 25 °C in an Eppendorf Thermomixer being shaken at 500 rpm. After 0.5, 2, 8, 32, 128, and 256 min, aliquots were withdrawn, and isotopic exchange was quenched by adding formic acid to a concentration of 0.5% (v/v), splitting the samples in triplicate, and freezing them in liquid nitrogen. Triplicates acted as controls for the reproducibility of the in-solution dissociation and digestion steps that were performed prior to analysis (explained below).

Mass Spectrometry. Samples were run using a Waters HDX-Manager (Waters Corp., Milford, MA), with a desalting flow of a 0.23% aqueous formic acid solution provided by an Agilent 1260 Infinity quaternary pump (Agilent Technologies, Santa Clara, CA) and a gradient flow provided by a nanoAcquity UPLC Binary Solvent Manager (Waters). For intact protein (global exchange) analysis, the quenched samples were thawed, adjusted to 35% (v/v) formic acid, and incubated on ice for 2 min to promote dissociation of aggregates. Gel filtrations indicated that this procedure was sufficient to dissociate the oligomers (Figure S1 of the Supporting Information). Samples were subsequently adjusted to pH 2.5 using 5.0 M NaOH and injected. A 700 μL/min desalting flow and a 50 μL/min gradient flow (5 to 50% B over 3 min) were used, along with a MassPREP Micro Desalting Column (Waters). For peptide (local exchange) analysis, samples were thawed and digested in solution using a large excess of pepsin [23:1 (w/w)] for 2 min prior to injection. A 500 μL/min desalting flow and a 40 μL/min gradient flow (8 to 40% B over 6 min) were used, along with a Zorbax Stablebond Guard Column and a 1.0 mm × 50 mm Zorbax Stablebond C18 column (Agilent Technologies). Samples were analyzed by ESI-MS using a Waters Synapt G1 mass spectrometer with a detector MCP voltage of 1700 V for intact proteins or 1950 V for peptides. Rigorous washing steps, consisting of three short gradients from 5 to 90% B, were performed between each injection. Blanks were recorded periodically, and signals arising from peptide carryover were found to be negligible.

Data Analysis. The identity of the peptic peptides was confirmed by LC−MS/MS analysis on an LTQ-Orbitrap mass spectrometer (Thermo Fisher Scientific, Waltham, MA). LTQ-Orbitrap raw data files were converted to Mascot generic format (MGF) files using Proteome Discoverer version 1.1 (Thermo Scientific, Franklin, MA) with default settings. MassAI 1.05 (MassAI Bioinformatics) was used to identify peptides from the MGF files. Deuterium incorporation was determined using DynamX version 0.8 (Waters). Gaussian fitting of isotopic distributions was done in Excel.

SDS−PAGE. Intact and digested αSN monomers and oligomers were run on a 4 to 20% tris-glycine polyacrylamide gel using a TGS buffer. All samples were mixed with 1:1 sample buffer (SDS and β-mercaptoethanol) and boiled for 10 min.

Antibody Blotting. Protein (monomeric or oligomeric, 250 ng per dot) was loaded onto a nitrocellulose membrane. The membrane was dried and stored until all time points were obtained. The membrane was developed as previously described with the Fila-1 antibody and anti-rabbit HRP (DAKO), stripped [100 mM glycine (pH 2.5)], and subsequently developed with the ASY-1 antibody and anti-rabbit HRP (DAKO).[29−31]

RESULTS

The αSN Oligomers Slowly Dissociate after Excess Monomer Is Removed. αSN oligomers were produced and isolated using gel filtration as previously described by Lashuel et al.[11] Removing the excess monomers and lowering the total αSN concentration in the solution shifted the equilibrium from oligomer association to dissociation, making the oligomers metastable as no stabilizing factors were present, e.g., metal ions[32,33] or covalent cross-linking to dopamine.[34] To examine the stability of the oligomers after they had been isolated, a fraction (0.5 mg/mL) was stored at 0 °C. Samples were drawn after 3 h (designated day 0), 7 days, and 14 days and analyzed in parallel by gel filtration and dot blotting. The isolated samples were centrifuged prior to being analyzed, and no indications of insoluble species could be observed, even after the samples had been stored for 21 days. The soluble oligomers were metastable with respect to dissociation, as evidenced by the increasing amount of monomeric αSN over time in the gel filtration chromatograms (Figure 1). Approximately 15%

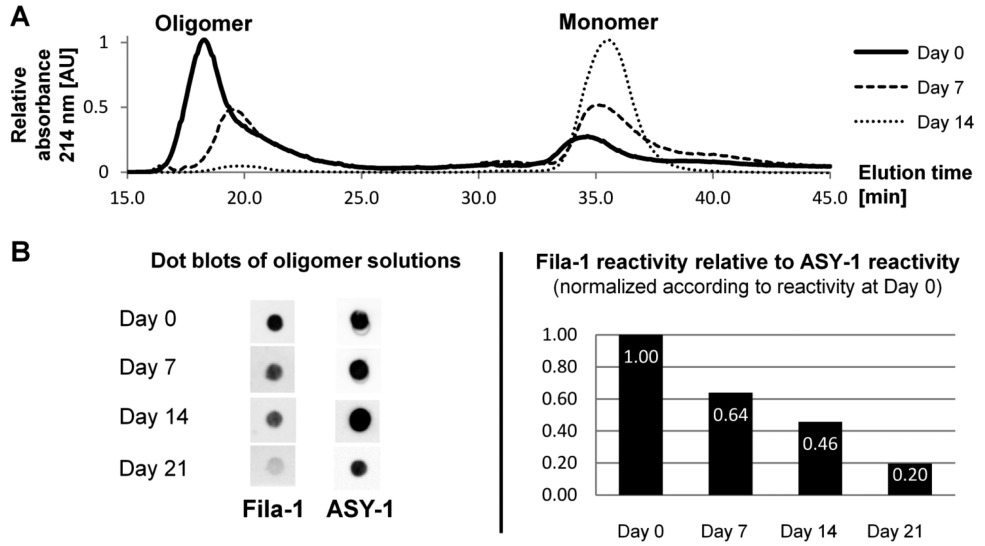

Figure 1. αSN oligomer stability analyzed by gel filtration and Fila-1 antibody reactivity. Oligomer and monomer samples were subjected to these analyses 3 h (day 0) and 7, 14, and 21 days after isolation. (A) Gel filtrations were performed to evaluate dissociation of oligomers to monomers. The peak at 18 min (day 0) corresponded to the elution time at which the oligomeric αSN was originally purified. (B) Dot blotting, probing for Fila-1 immunoreactivity in samples containing approximately 250 ng of total αSN. Monomeric αSN was used as a negative control. To check αSN loading, filters were stripped for Fila-1 IgG and reprobed with the anti-ASY-1 antibody that binds both monomeric and aggregated αSN. Fila-1 reactivity is given relative to the observed ASY-1 reactivity, to compensate for variations in the amounts of protein loaded.

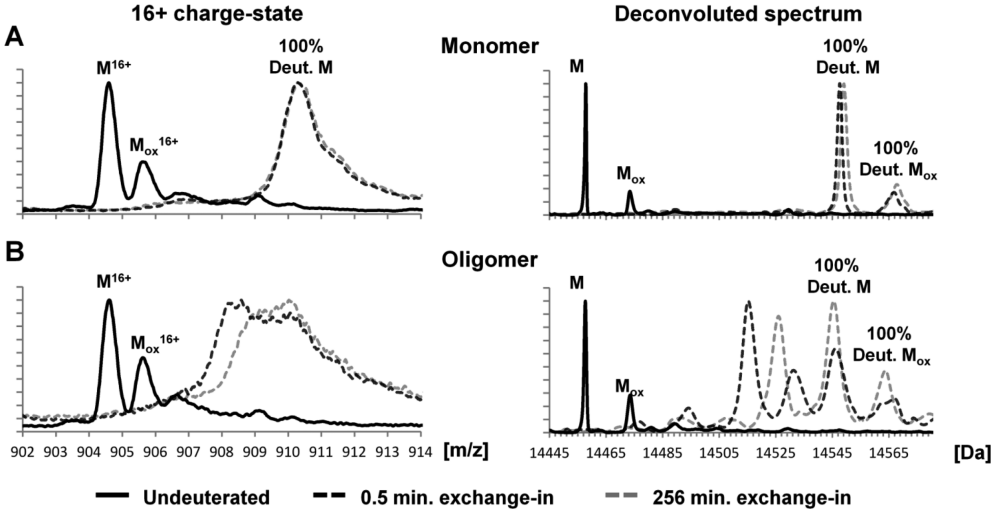

Figure 2. Global exchange profiles for αSN monomers and oligomers comparing their undeuterated state and deuterium incorporation after exchange for 0.5 and 256 min. Spectra represent the most abundant charge state (+16) and the deconvoluted spectrum. Peaks labeled M denote the molecular mass of the protein, while peaks labeled M_{ox} denote oxidation products. (A) Deuterated monomeric αSN gave rise to a single unprotected population, exhibiting a mass increase of ~90 Da after exchange for 0.5 min. (B) Deuterated oligomeric αSN gave rise to two populations (i.e., protected αSN and unprotected αSN), with the unprotected population behaving like the monomer and the protected population displaying a mass increase of ~58 Da after exchange for 0.5 min. Spectra were deconvoluted using MaxEnt 1. The raw mass spectra presented here were smoothed.

monomeric αSN could be observed after 3 h, representing a relatively fast initial dissociation phase. This tendency continued, albeit at a lower rate, with approximately 60% of the signal belonging to the monomer peak after 7 days and 95% after 14 days. Interestingly, the oligomers analyzed after the samples had been stored for 7 and 14 days eluted later, i.e., at smaller hydrodynamic volumes, suggesting that they had become smaller (Figure 1A).

The rabbit polyclonal aggregation-specific antibody, Fila-1, is raised against insoluble αSN fibrils and depleted for αSN monomer reactivity and has previously been used to detect insoluble fibrils and soluble oligomers of αSN.[30,31] Dot blot analysis, examining the stability of the oligomers using Fila-1, displayed a surprisingly slower decay compared to the loss of oligomer content when analyzed by gel filtration (Figure 1B); 64% of the Fila-1 reactivity present at day 0 was retained after 7 days and 46% after 14 days, despite the intensity of the oligomer peak being reduced to approximately 40 and 5% in the gel filtration chromatograms. The Fila-1 reactivity was further reduced to 20% after the oligomers had been stored for 21 days.

Unless otherwise stated, the oligomers characterized in this study were stored for 2 days at 0 °C before HDX analysis. Qualitatively, the exchange patterns observed in the day 0 samples (i.e., storage for 3 h) were nearly identical to those of day 2 samples (Figure S1 of the Supporting Information).

dx.doi.org/10.1021/bi4009193 | *Biochemistry* 2013, 52, 9097−9103

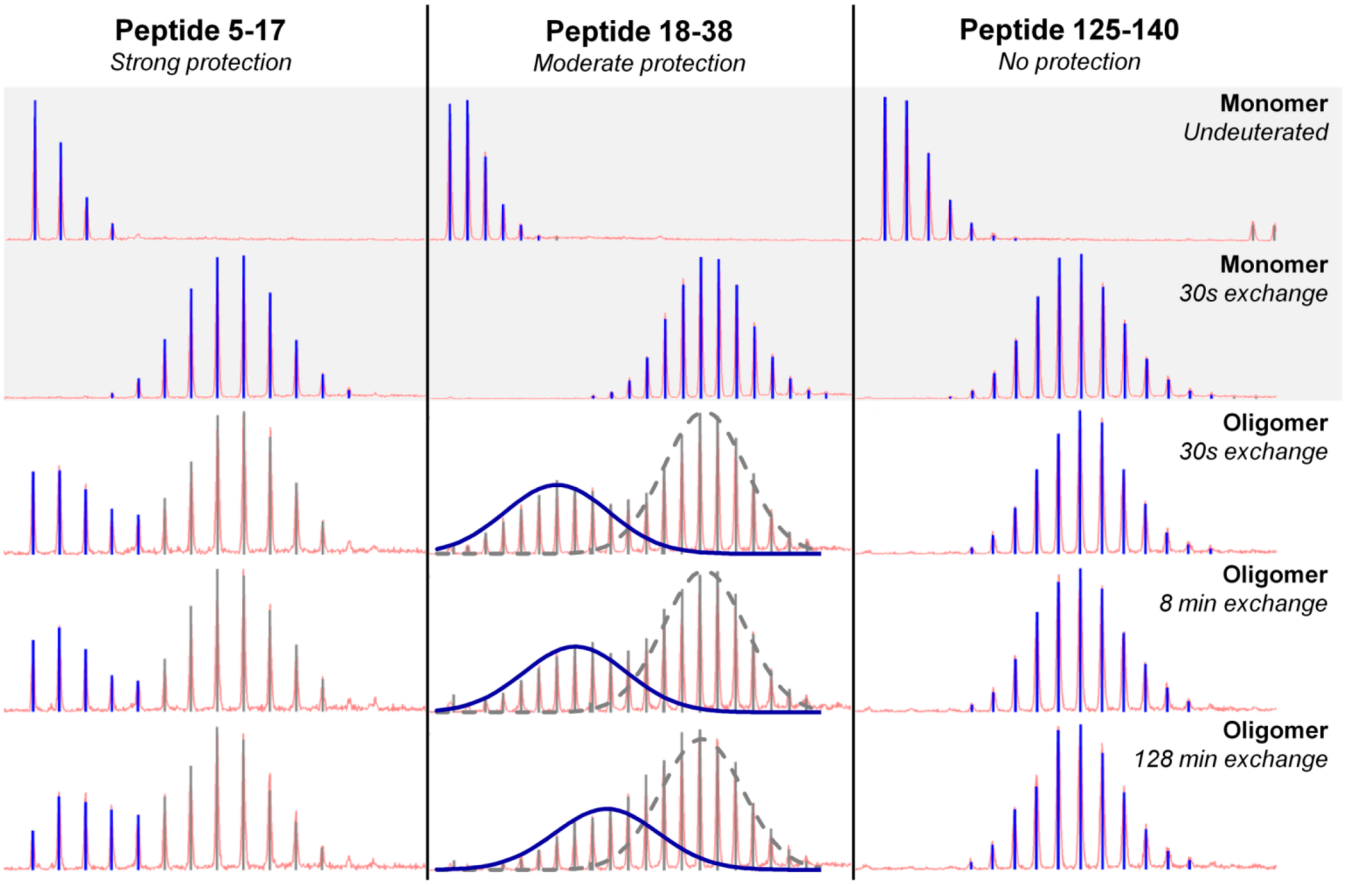

Figure 3. Examples of local exchange profiles for three representative peptides exhibiting strong (left), moderate (middle), and weak or no protection (right). For each peptide, spectra are shown for the undeuterated monomer, the monomer preparation after exchange for 0.5 min, and the oligomer preparation after exchange for 0.5, 8, and 128 min. Isotopic distributions highlighted in blue were used in quantifying the deuterium content of the peptides.

H/D Exchange Measurements Show That αSN Oligomers Are Protected against Isotopic Exchange. Prior to intact protein analysis, monomer and oligomer solutions were both subjected to dissociation by incubation in 35% formic acid for 2 min. Acidified samples were subsequently adjusted to pH 2.5 using 5 M NaOH and immediately injected. This procedure was found to increase the level of back-exchange by ∼6%, upon comparison to the deuterium content of labeled αSN monomers with and without the dissociation procedure (data not shown). For monomer and oligomer preparations, a base peak (14460.9 Da) matching the theoretical mass of αSN (14460.2 Da) was observed in the undeuterated samples (Figure 2). No peaks from, for example, contaminating proteins or truncated αSN were present. However, peaks corresponding to an oxidation product could be observed. The backbone amides in monomeric αSN are known to exchange at rates very close to their intrinsic chemical exchange rates, in accordance with the absence of any stable structure in monomeric αSN (intrinsically disordered state).[27] According to the predicted intrinsic chemical exchange rates for αSN under these experimental conditions, the exchange will be complete (99.9%) after deuteration for 10 s. Similarly, our experimental HDX data for monomeric αSN show no sign of any stable structure as the deuterium uptake is complete after the shortest period of deuteration [i.e., at 0.5 min (see Figure 2A)]. αSN exhibited a 26% loss of deuterium due to back-exchange under quench conditions. For the deuterated oligomeric sample, the deconvoluted mass spectra show four major peaks that correspond to two populations (i.e., protected αSN and unprotected αSN), as each population is split into two peaks because of the presence of oxidized αSN (Figure 2B). The HDX profile of the unprotected αSN population closely matches that of the monomeric αSN sample in Figure 2A, while the protected population appears at a lower mass, indicating a stable structure that exhibits protection of some of its backbone amides. The protected backbone amides incorporated additional deuterium during prolonged isotopic exchange (256 min). Interestingly, the peak widths of the populations obtained from the oligomer preparation were significantly broader than those obtained from the monomeric sample. This could be an indication of slight structural heterogeneity and would correspond well with previous reports of oligomer heterogeneity in identical preparations made by Lashuel et al.[11] The presence of unprotected αSN in the oligomer preparation corresponded well with the dissociation we observed when we performed subsequent gel filtrations on the isolated oligomers.

Spatially Resolved H/D Exchange Shows That the N-Terminus Is Protected against Isotopic Exchange in αSN Oligomers. The labeled preparations were also analyzed at the peptide level by digesting the deuterated samples with pepsin prior to LC−MS analysis. SDS−PAGE of digested monomeric and oligomeric αSN (undeuterated) revealed that no intact protein remained after such treatment, indicating that our

dx.doi.org/10.1021/bi4009193 | Biochemistry 2013, 52, 9097−9103

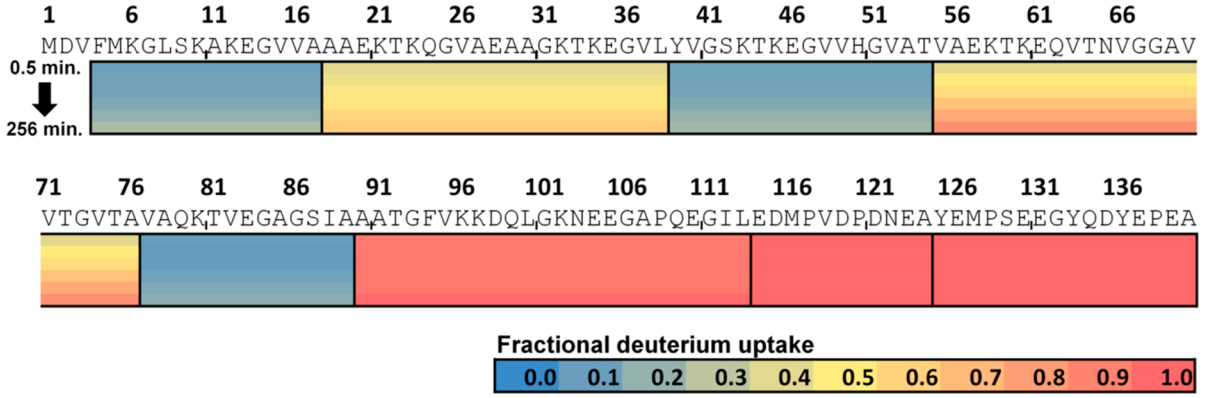

Figure 4. Heat map of the local exchange patterns observed in peptides derived from deuterium-labeled αSN oligomers. For the sake of simplicity, only nonoverlapping peptides are shown. A heat map that includes all identified peptides can be found in Figure S9 of the Supporting Information. Peptides are color-coded according to fractional deuterium uptake, relative to peptides derived from the fully exchanged αSN monomers. The coloring of each peptide, from top to bottom, represents deuterium uptake after exchange for 0.5, 2, 8, 32, 128, and 256 min.

analysis sampled all of the aggregation states present in the oligomer preparation (Figure S3 of the Supporting Information). Representative spectra exemplifying the observed deuteration patterns are shown in Figure 3. Peptides derived from the αSN monomers did not exhibit any sign of backbone amide protection, all being fully exchanged after they had been labeled for 0.5 min and all giving rise to uniform Gaussian isotopic distributions (Figure 3 and Figure S7 of the Supporting Information). This fits our observations of intact monomeric αSN, where exchange was also complete after samples had been labeled for 0.5 min.

The deuterated preparations of oligomeric αSN gave rise to peptide mass spectra that contained one or two distinct isotopic distributions (Figure 3, bottom). Isotopic distributions corresponding to the fully deuterated peptide, identical to those observed in the monomer preparation, could be observed in all peptide spectra. The universal presence of ions representing an unstructured state is in accordance with the global exchange results obtained for oligomeric αSN. For most peptides, the unstructured conformer was accompanied by an isotopic distribution containing fewer deuterons, representing a structured conformer exhibiting protection from isotopic exchange in its backbone amides. We employed three different metrics to quantify the deuterium content of these protected conformers, based on how much their isotopic envelopes overlapped with those of the fully deuterated peptides. Where the two distributions were clearly separate, only the isotopic envelope with the lowest deuterium content was used to calculate the deuterium content of the protected conformer (Figure 3, peptide 5−17). Where the isotopic envelopes belonging to the protected and the monomeric conformer did overlap, a Gaussian fitting procedure was performed to determine the average deuterium content of the protected conformer (Figure 3, peptide 18−38). Where only a single isotopic envelope was present, this was expected to represent the deuterium content of both conformers in the solution; i.e., the protected conformer mirrored the unstructured monomeric conformer in this region (Figure 3, peptide 125−140). The raw mass spectra for peptides 5−17, 18−38, and 125−140, covering the entire exchange series, can be found in Figures S4−S6 of the Supporting Information. Deuterium uptake plots, comparing deuterium incorporation in the monomeric and oligomeric samples for each peptide, can be found in Figure S7 of the Supporting Information.

A heat map overview of deuterium uptake in the protected oligomeric state, normalized according to deuterium uptake in the fully exchanged monomeric state, can be found in Figure 4. The C-terminus of αSN, starting at amino acid 94, appears to be unstructured and thus fully solvent accessible in the oligomers, exchanging completely within 0.5 min of exchange. Within the larger region of residues 1−95 of αSN, containing 6 of the 11-mer consensus repeats,[35] it is interesting to note the three protected regions of approximately 14 amino acids (4−17, 39−54, and 70−89), which are interspersed with two more dynamic regions (18−38 and 55−76). It was not surprising that the region of residues 70−89 was protected, given that it is a part of the hydrophobic NAC domain, spanning amino acids 61−95.[35] We expect that the fast-exchanging backbone amides of peptide 55−76 are located in the region of residues 55−70, as peptide 70−89 was also found to exchange very slowly (Figure S8 of the Supporting Information).

DISCUSSION

Interestingly, the deuteration pattern we observe for αSN in the oligomers has only slight indications of heterogeneity, both at the intact protein level and at the peptide level. Such a lack of heterogeneity is a good indication that the oligomers are ordered assemblies, perhaps varying in size. The N-terminal protection we observe in the oligomeric state probed in this study is particularly interesting, as previous HDX-MS and -NMR analyses of αSN in its monomeric and fibrillar states showed the N-terminus to exchange rapidly.[27,28] The ability of peptide 55−76 to undergo isotopic exchange in the oligomeric state is also distinctly different from observations in fibrils studied by HDX-NMR, which contained a continuous protected region from amino acid 39 to 97.[27] The strongly protected regions we observe in our oligomer preparation, i.e., peptides 39−54 and 70−89, along with the less protected region of residues 55−70, match the behavior one would expect if these two regions formed elongated β-strands, as has been proposed for αSN fibrils based on NMR and electron paramagnetic resonance (EPR) measurements.[36,37] It is possible that the analyzed oligomers adopt a similar fold, although the β-strands would appear to be less elongated, approximately 20 residues compared to the 26−30 residues reported for the fibrils. Such similar folds, with the oligomers exhibiting extended dynamic regions and shortened ordered regions compared to fibril models, could indicate a zipperlike

dx.doi.org/10.1021/bi4009193 | Biochemistry 2013, 52, 9097−9103

maturation process that would shield larger parts of the 11-mer αSN consensus repeats as aggregation progressed. It should be noted that the HDX-NMR analyses performed by Vilar et al. matched a fibrillar model in which αSN adopted a structure containing five stacked antiparallel β-strands.[28]

Throughout the study, we observe a difference in the relative abundance of monomeric and oligomeric αSN when comparing our HDX data with gel filtration chromatograms and antibody plots. The mass spectra for the deuterated αSN oligomer preparation indicated that a larger amount of monomers were present, compared to gel filtration chromatograms (Figures 1A and 2B). This difference is likely due to batch-to-batch variations as the results presented in Figure 1 and 2 arise from two different batches of αSN oligomers. Additionally, we speculate about whether oligomeric peripherally associated αSN eluting in the oligomer fraction could have a flexible structure that would exchange completely within 0.5 min.

Quantitative differences were also observed upon comparison of oligomer and monomer abundance in the same preparation, using gel filtration and Fila-1 reactivity. Interestingly, similar quantitative differences in oligomer/monomer ratios as measured by gel filtration and other techniques (SAXS, DLS, and NMR) have previously been reported for αSN oligomers.[14,38,39] In these cases, interactions with the gel filtration resin were proposed as likely causes for the discrepancies, with resin interactions promoting the dissociation of the oligomers. Taken together, the Fila-1 and gel filtration data suggest that the oligomers that remain in the solution after being stored for 14 days are still capable of binding Fila-1, but a large proportion of the oligomers dissociate upon gel filtration.

While subsequent gel filtrations and antibody blotting indicate that the isolated oligomers were metastable with respect to dissociation over a period of weeks (Figure 1), the oligomers were stable on the time scale of the labeling. This is exemplified by the fully exchanged state being equally abundant after exchange for 0.5 and 256 min (see examples in Figures S4 and S5 of the Supporting Information; other peptides exhibit the same characteristics but are not shown).

On the basis of our observations, it would be very interesting to investigate whether the N-terminal structuring of αSN we observe is also present in oligomers formed by wt αSN in the presence of additives that promote aggregation, or in oligomers formed by the αSN point mutants leading to autosomal dominant forms of PD. Further studies to probe the oligomeric structure of αSN and variants thereof using HDX-MS and other approaches such as limited proteolysis will be pursued.

In conclusion, HDX-MS analysis was able to successfully identify a protected structure of oligomeric αSN from a solution containing oligomers generated using wt αSN, in the absence of aggregation promoting or stabilizing additives. This represents the first analysis of αSN backbone dynamics upon adoption of a soluble, oligomeric state. We believe that this method would be able to compare differences in aggregate heterogeneity or conformation for oligomers generated under different conditions or using different mutants of αSN. Such analyses could potentially lead to a more detailed understanding of the formation and function of αSN oligomers.

■ ASSOCIATED CONTENT

Supporting Information

Comparison of deuterium uptake in day 0 and day 2 oligomers after exchange for 30 s (Figure S1), analysis of αSN oligomer dissociation using gel filtration chromatography (Figure S2), SDS−PAGE analysis of in-solution digestion of αSN monomers and oligomers (Figure S3), representative spectra illustrating deuterium uptake in peptides 5−17, 18−38, and 125−140 from monomer and oligomer preparations (Figures S4−S6), deuterium uptake plots for each individual peptide identified in the monomeric and oligomeric αSN preparations (Figure S7), and an expanded heat map of the local exchange patterns observed in peptides derived from deuterium-labeled αSN oligomers (Figure S8). This material is available free of charge via the Internet at http://pubs.acs.org.

■ AUTHOR INFORMATION

Corresponding Author

*Phone: +45 6550 2409. E-mail: tjdj@bmb.sdu.dk.

Funding

We gratefully acknowledge financial support by the Lundbeck Foundation, Denmark (Grant 95-310-13595, S.M.). This work was also supported by a grant from The Carlsberg Foundation (T.J.D.J.).

Notes

The authors declare no competing financial interest.

■ ABBREVATIONS

αSN, α-synuclein; AFM, atomic force microscopy; EM, electron microscopy; EPR, electron paramagnetic resonance; HDX, hydrogen/deuterium exchange; LC, liquid chromatography; MS, mass spectrometry; NAC, non-amyloid-β component; NMR, nuclear magnetic resonance; PAGE, polyacrylamide gel electrophoresis; PD, Parkinson's disease; PBS, phosphate-buffered saline; SAXS, small-angle X-ray scattering; SDS, sodium dodecyl sulfate; TGS, Tris-glycine-SDS.

■ REFERENCES

(1) Lang, A. E., and Lozano, A. M. (1998) Parkinson's disease: First of two parts. *N. Engl. J. Med. 339*, 1044−1053.

(2) Caughey, B., and Lansbury, P. T. (2003) Protofibrils, pores, fibrils, and neurodegeneration: Separating the responsible protein aggregates from the innocent bystanders. *Annu. Rev. Neurosci. 26*, 267−298.

(3) Polymeropoulos, M. H., Lavedan, C., Leroy, E., Ide, S. E., Dehejia, A., Dutra, A., Pike, B., Root, H., Rubenstein, J., Boyer, R., Stenroos, E. S., Chandrasekharappa, S., Athanassiadou, A., Papapetropoulos, T., Johnson, W. G., Lazzarini, A. M., Duvoisin, R. C., DiIorio, G., Golbe, L. I., and Nussbaum, R. L. (1997) Mutation in the α-synuclein gene identified in families with Parkinson's disease. *Science 276*, 2045−2047.

(4) Kruger, R., Kuhn, W., Muller, T., Woitalla, D., Graeber, M., Kosel, S., Przuntek, H., Epplen, J. T., Schols, L., and Riess, O. (1998) Ala30Pro mutation in the gene encoding α-synuclein in Parkinson's disease. *Nat. Genet. 18*, 106−108.

(5) Zarranz, J. J., Alegre, J., Gomez-Esteban, J. C., Lezcano, E., Ros, R., Ampuero, I., Vidal, L., Hoenicka, J., Rodriguez, O., Atares, B., Llorens, V., Tortosa, E. G., del Ser, T., Munoz, D. G., and de Yebenes, J. G. (2004) The new mutation, E46K, of α-synuclein causes Parkinson and Lewy body dementia. *Ann. Neurol. 55*, 164−173.

(6) Appel-Cresswell, S., Vilarino-Guell, C., Yu, I., Shah, B., Weir, D., Thompson, C., Stoessl, J. A., and Farrer, M. J. (2012) α-Synuclein H50Q, a novel pathogenic mutation for Parkinson's disease. *Mov. Disord. 27*, S447.

(7) Lesage, S., Anheim, M., Letournel, F., Bousset, L., Honore, A., Rozas, N., Pieri, L., Madiona, K., Durr, A., Melki, R., Verny, C., and Brice, A. (2013) G51D α-synuclein mutation causes a novel parkinsonian-pyramidal syndrome. *Ann. Neurol.*, DOI: 10.1002/ana.23894.

(8) Hoffman-Zacharska, D., Koziorowski, D., Ross, O. A., Milewski, M., Poznański, J., Jurek, M., Wszolek, Z. K., Soto-Ortolaza, A., Sławek, J., Janik, P., Jamrozik, Z., Potulska-Chromik, A., Jasińska-Myga, B., Opala, G., Krygowska-Wajs, A., Czyżewski, K., Dickson, D. W., Bal, J., and Friedman, A. (2013) Novel A18T and pA29S substitutions in α-synuclein may be associated with sporadic Parkinson's disease. *Parkinsonism and Related Disorders 19*, 1057−1060.
(9) Conway, K. A., Harper, J. D., and Lansbury, P. T. (1998) Accelerated in vitro fibril formation by a mutant α-synuclein linked to early-onset Parkinson disease. *Nat. Med. 4*, 1318−1320.
(10) Bertoncini, C. W., Jung, Y. S., Fernandez, C. O., Hoyer, W., Griesinger, C., Jovin, T. M., and Zweckstetter, M. (2005) Release of long-range tertiary interactions potentiates aggregation of natively unstructured α-synuclein. *Proc. Natl. Acad. Sci. U.S.A. 102*, 1430−1435.
(11) Lashuel, H. A., Petre, B. M., Wall, J., Simon, M., Nowak, R. J., Walz, T., and Lansbury, P. T. (2002) α-Synuclein, especially the Parkinson's disease-associated mutants, forms pore-like annular and tubular protofibrils. *J. Mol. Biol. 322*, 1089−1102.
(12) Apetri, M. M., Maiti, N. C., Zagorski, M. G., Carey, P. R., and Anderson, V. E. (2006) Secondary structure of α-synuclein oligomers: Characterization by Raman and atomic force microscopy. *J. Mol. Biol. 355*, 63−71.
(13) Conway, K. A., Lee, S. J., Rochet, J. C., Ding, T. T., Williamson, R. E., and Lansbury, P. T. (2000) Acceleration of oligomerization, not fibrillization, is a shared property of both α-synuclein mutations linked to early-onset Parkinson's disease: Implications for pathogenesis and therapy. *Proc. Natl. Acad. Sci. U.S.A. 97*, 571−576.
(14) Giehm, L., Svergun, D. I., Otzen, D. E., and Vestergaard, B. (2011) Low-resolution structure of a vesicle disrupting α-synuclein oligomer that accumulates during fibrillation. *Proc. Natl. Acad. Sci. U.S.A. 108*, 3246−3251.
(15) Katta, V., and Chait, B. T. (1991) Conformational Changes in Proteins Probed by Hydrogen Exchange Electrospray-Ionization Mass Spectrometry. *Rapid Commun. Mass Spectrom. 5*, 214−217.
(16) Zhang, Z. Q., and Smith, D. L. (1993) Determination of Amide Hydrogen Exchange by Mass Spectrometry: A New Tool for Protein-Structure Elucidation. *Protein Sci. 2*, 522−531.
(17) Wales, T. E., and Engen, J. R. (2006) Hydrogen exchange mass spectrometry for the analysis of protein dynamics. *Mass Spectrom. Rev. 25*, 158−170.
(18) Kheterpal, I., Chen, M., Cook, K. D., and Wetzel, R. (2006) Structural differences in Aβ amyloid protofibrils and fibrils mapped by hydrogen exchange: Mass spectrometry with on-line proteolytic fragmentation. *J. Mol. Biol. 361*, 785−795.
(19) Kheterpal, I., Lashuel, H. A., Hartley, D. M., Wlaz, T., Lansbury, P. T., and Wetzel, R. (2003) Aβ protofibrils possess a stable core structure resistant to hydrogen exchange. *Biochemistry 42*, 14092−14098.
(20) Kheterpal, I., Zhou, S., Cook, K. D., and Wetzel, R. (2000) Aβ amyloid fibrils possess a core structure highly resistant to hydrogen exchange. *Proc. Natl. Acad. Sci. U.S.A. 97*, 13597−13601.
(21) Alexandrescu, A. T. (2013) Amide Proton Solvent Protection in Amylin Fibrils Probed by Quenched Hydrogen Exchange NMR. *PLoS One 8*, No. e56467.
(22) Carulla, N., Zhou, M., Arimon, M., Gairi, M., Giralt, E., Robinson, C. V., and Dobson, C. M. (2009) Experimental characterization of disordered and ordered aggregates populated during the process of amyloid fibril formation. *Proc. Natl. Acad. Sci. U.S.A. 106*, 7828−7833.
(23) Carulla, N., Zhou, M., Giralt, E., Robinson, C. V., and Dobson, C. M. (2010) Structure and Intermolecular Dynamics of Aggregates Populated during Amyloid Fibril Formation Studied by Hydrogen/Deuterium Exchange. *Acc. Chem. Res. 43*, 1072−1079.
(24) Vilar, M., Wang, L., and Riek, R. (2012) Structural studies of amyloids by quenched hydrogen-deuterium exchange by NMR. *Methods Mol. Biol. 849*, 185−198.
(25) Carulla, N., Caddy, G. L., Hall, D. R., Zurdo, J., Gairi, M., Feliz, M., Giralt, E., Robinson, C. V., and Dobson, C. M. (2005) Molecular recycling within amyloid fibrils. *Nature 436*, 554−558.
(26) Cho, M. K., Kim, H. Y., Fernandez, C. O., Becker, S., and Zweckstetter, M. (2011) Conserved core of amyloid fibrils of wild type and A30P mutant α-synuclein. *Protein Sci. 20*, 387−395.
(27) Del Mar, C., Greenbaum, E. A., Mayne, L., Englander, S. W., and Woods, V. L. (2005) Structure and properties of α-synuclein and other amyloids determined at the amino acid level. *Proc. Natl. Acad. Sci. U.S.A. 102*, 15477−15482.
(28) Vilar, M., Chou, H. T., Luhrs, T., Maji, S. K., Riek-Loher, D., Verel, R., Manning, G., Stahlberg, H., and Riek, R. (2008) The fold of α-synuclein fibrils. *Proc. Natl. Acad. Sci. U.S.A. 105*, 8637−8642.
(29) Colla, E., Jensen, P. H., Pletnikova, O., Troncoso, J. C., Glabe, C., and Lee, M. K. (2012) Accumulation of Toxic α-Synuclein Oligomer within Endoplasmic Reticulum Occurs in α-Synucleinopathy In Vivo. *J. Neurosci. 32*, 3301−3305.
(30) Lindersson, E., Beedholm, R., Hojrup, P., Moos, T., Gai, W. P., Hendil, K. B., and Jensen, P. H. (2004) Proteasomal inhibition by α-synuclein filaments and oligomers. *J. Biol. Chem. 279*, 12924−12934.
(31) Paleologou, K. E., Kragh, C. L., Mann, D. M. A., Salem, S. A., Al-Shami, R., Allsop, D., Hassan, A. H., Jensen, P. H., and El-Agnaf, O. M. A. (2009) Detection of elevated levels of soluble α-synuclein oligomers in post-mortem brain extracts from patients with dementia with Lewy bodies. *Brain 132*, 1093−1101.
(32) Danzer, K. M., Haasen, D., Karow, A. R., Moussaud, S., Habeck, M., Giese, A., Kretzschmar, H., Hengerer, B., and Kostka, M. (2007) Different species of α-synuclein oligomers induce calcium influx and seeding. *J. Neurosci. 27*, 9220−9232.
(33) Kostka, M., Hogen, T., Danzer, K. M., Levin, J., Habeck, M., Wirth, A., Wagner, R., Glabe, C. G., Finger, S., Heinzelmann, U., Garidel, P., Duan, W., Ross, C. A., Kretzschmar, H., and Giese, A. (2008) Single particle characterization of iron-induced pore-forming α-synuclein oligomers. *J. Biol. Chem. 283*, 10992−11003.
(34) Conway, K. A., Rochet, J. C., Bieganski, R. M., and Lansbury, P. T. (2001) Kinetic stabilization of the α-synuclein protofibril by a dopamine-α-synuclein adduct. *Science 294*, 1346−1349.
(35) Ueda, K., Fukushima, H., Masliah, E., Xia, Y., Iwai, A., Yoshimoto, M., Otero, D. A. C., Kondo, J., Ihara, Y., and Saitoh, T. (1993) Molecular Cloning of cDNA Encoding an Unrecognized Component of Amyloid in Alzheimer's Disease. *Proc. Natl. Acad. Sci. U.S.A. 90*, 11282−11286.
(36) Chen, M., Margittai, M., Chen, J., and Langen, R. (2007) Investigation of α-synuclein fibril structure by site-directed spin labeling. *J. Biol. Chem. 282*, 24970−24979.
(37) Comellas, G., Lemkau, L. R., Nieuwkoop, A. J., Kloepper, K. D., Ladror, D. T., Ebisu, R., Woods, W. S., Lipton, A. S., George, J. M., and Rienstra, C. M. (2011) Structured Regions of α-Synuclein Fibrils Include the Early-Onset Parkinson's Disease Mutation Sites. *J. Mol. Biol. 411*, 881−895.
(38) Bhak, G., Lee, J. H., Hahn, J. S., and Paik, S. R. (2009) Granular Assembly of α-Synuclein Leading to the Accelerated Amyloid Fibril Formation with Shear Stress. *PLoS One 4*, No. e4177.
(39) Horvath, I., Weise, C. F., Andersson, E. K., Chorell, E., Sellstedt, M., Bengtsson, C., Olofsson, A., Hultgren, S. J., Chapman, M., Wolf-Watz, M., Almqvist, F., and Wittung-Stafshede, P. (2012) Mechanisms of Protein Oligomerization: Inhibitor of Functional Amyloids Templates α-Synuclein Fibrillation. *J. Am. Chem. Soc. 134*, 3439−3444.